PostDoc Journal
Vol. 6, No. 1, January 2018

Journal of Postdoctoral Research
www.postdocjournal.com

6-Mercaptopurine Nucleoside Complexes of Gold(I): Synthesis and Cytotoxicity

Ayan Maity,[a]* Nihal Deligonul,[b] Anthony J. Berdis[c,]* and Thomas G. Gray[b]
[a]Department of Chemistry, Massachusetts Institute of Technology, Cambridge, MA 02139, USA
[b]Department of Chemistry, Case Western Reserve University, 10900 Euclid Avenue, Cleveland, Ohio 44106, USA
[c]Department of Chemistry, Center for Gene Regulation in Health and Disease, Cleveland State University, Cleveland, Ohio 44115, USA
Email: amaity@mit.edu

ABSTRACT
Molecular gold compounds have shown intermittent promise as human pharmaceuticals, mostly in *in vitro* assays. Rational approaches to gold prodrugs are essential for desired cytotoxicity. This work describes non-natural nucleosides of 6-mercaptopurine. Binding to (organophosphine)- and (*N*-heterocyclic carbene)gold(I) proceeds in high-yield reactions at room temperature. Three such metallonucleosides were prepared. They differ in the phosphine or carbene ligand on gold. New compounds are characterized by multinuclear NMR spectroscopy, mass spectrometry, and elemental analysis. One complex is crystallographically characterized; gold(I) is bound to the sulfur atom of the mercaptopurine moiety, and aurophilic interactions are absent. Experiments in human cell lines showed evidence of mitochondrial swelling, programmed cell death, and inhibition of rat liver thioredoxin reductase.

1. INTRODUCTION

The modern chemistry of gold drugs was born in the treatment of rheumatoid arthritis. *Auranofin* is a (phosphine)gold(I) prodrug developed as an orally available anti-arthritic drug (Figure 1).[1–7] Despite promising early results, injectable forms of gold(I) proved more effective, and auranofin's use in arthritis therapy has tapered. More recent interest derives from observations of its anti-cancer activity. Research in the late 1970s and early 1980s showed that auranofin inhibits the growth of tumor cells in culture. Auranofin is also active *in vivo* against one mouse tumor model (mouse lymphocytic leukemia P388).[8–12] These findings, alongside burgeoning studies of platinum metallodrugs, have drawn attention to the bio-

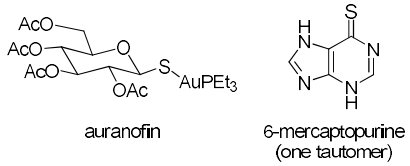

Figure 1. Structure of Auranofin and 6-mercaptopurine

chemistry of gold. Today, medicinal gold chemistry targets cancers, AIDS, malaria, and other diseases.[13] Ongoing concerns are the design of gold pharmacophores,[14] the effects of oxidation state, and selectivity toward protein targets.

Berners-Price,[15] Nolan,[16] and their respective coworkers have reported analogues of auranofin with *N*-heterocyclic carbene (NHC) ligands in place of triethylphosphine. These compounds avoid any toxicity associated with phosphine ligands. A family of gold(I) bis(*N*-heterocyclic carbene) complexes has been characterized biologically.[17–19] The *N*-substituents on the carbene ligands alter their lipophilicities. At least some such cations target malignant over normal cells.[20] Again, substitution at nitrogen controls selectivity and potency. Cell death occurs through mitochondrial apoptosis, and inhibition of a selenoenzyme, mitochondrial thioredoxin reductase (TrxR), is implicated.

Ott and co-workers[21] have examined three gold(I) complexes bearing benzimidazolylidene-type NHC ligands; two are cations. Positive charge promotes cellular uptake. Some structure-activity relationships are apparent within the three complexes. These (carbene)gold(I) species induce apoptosis and exert antiproliferative effects on two adherent cell lines. One gold(I) cation shows high mitochondrial uptake, and all three inhibit mitochondrial thioredoxin reductase. Another recent work[22] considers (NHC)gold bromides. In these complexes, the carbene ligands derive from 4,5-diarylimidazoles. Eleven gold(I) and two gold(III) complexes are examined. Growth of three cancer cell lines was impeded, and the new compounds inhibited rat liver mitochondrial thioredoxin

reductase. However, IC_{50} values are 1–2 orders of magnitude higher than for auranofin, suggesting that these two complexes target sites other than thioredoxin reductase.

Two-coordinate gold(I) undergoes associative substitution with thiols.[23] A series of gold(I) bis(phosphine) complexes were prepared, of which [bis(1,2-diphenylphosphinoethane)]gold(I), $[(dppe)_2Au]^+$, is the prototype.[24–27] This compound and related cations show an unusual tetrahedral (four-coordinate) geometry of gold(I) in the solid state. These compounds are less reactive toward protein thiols than auranofin. The cation $[(dppe)_2Au]^+$ is prohibitively toxic, but complexes of *o*-pyridyl phosphines are less so, with a favorable balance of lipophilicity and antitumor activity.[28] These gold(I) cations collect inside mitochondria, as a result of the mitochondrial membrane potential.[29,30] Selectivity is observed for malignant over normal breast cells. Cell death is apoptotic. Water-soluble analogues appeared recently. These inhibit the enzymes glutathione reductase and thioredoxin reductase and induce apoptosis.[31]

Theraputic properties of gold(I) were known from ages. In recent years, gold(III) has gained pharmacological attention, despite its reducibility by ascorbate, glutathione, and other endogenous reductants. Messouri and collaborators have devised a number of cytotoxic gold(III) complexes.[32–37] The metal centers are square planar, as expected for four-coordinate, low-spin d^8. These complexes include dinuclear, μ-oxo bridged 2,2′-bipyridine chelates; the most reducible is also the most toxic. The gold(III) dithiocarbamates of Fregona and co-workers inhibit the growth of breast cancer xenografts in mouse models.[38–41] These dithiocarbamate complexes are effective against cisplatin-resistant cell lines. Over the last decade, the Che group has developed cyclometalated gold(III) complexes that are toxic toward carcinoma cell lines.[42–44] In some instances, IC_{50} values are in the tens of nM. Cytotoxicity improves when two gold(III) centers are tethered with bridging diphosphine ligands. Che and co-workers have also assayed the toxicity of gold(III) *meso*-tetraarylporphyrins.[45–47] Gold(III) *meso*-tetraarylporphyrin chloride is not reduced in serum. Gold(III) porphyrins behave physically as delocalized lipophilic cations, much like gold(I) bis(carbene) or bis(diphosphine) species. Cell death results from apoptosis; both caspase-dependent and -independent pathways are proposed. Decorating the porphyrin rim with –OH substituents brings about potent activity against breast carcinoma cells. Cytotoxic effects appear at nanomolar concentrations.[48]

Few gold drugs target DNA. Proteins and enzymes that bind gold have been reviewed.[49] They divide into two broad categories: proteins with activated cysteine residues and those with selenocysteine. "Activated" cysteines are deprotonated by a nearby base, often histidine. They exist as the cysteine thiolate at physiological pH, although the normal pK_a of cysteine is 8.4. Selenocysteine is more acidic: pK_a 5.2. Both are strong nucleophiles that attack unhindered, electrophilic gold(I). Enzymes inhibited by gold include cathepsins,[50–53] human glutathione reductase,[54,55] poly(ADP-ribose) polymerase,[56] and protein tyrosine phosphatases.[57] All these are cysteinyl enzymes. Selenoenzyme targets are glutathione peroxidase,[58–63] iodothyronine diiodinase,[64,65] and thioredoxin reductase.[55,66–70] There are cytosolic (TrxR1) and mitochondrial (TrxR2) isoforms of thioredoxin reductase. In mammals, both have redox-active selenocysteine residues.

Mitochondria are the locus of auranofin's action in cell cultures. Treatment of immortalized cells with gold(I) leads to mitochondrial swelling, and intrisic (mitochondrial) apoptosis follows. Partly for these reasons, mitochondrial thioredoxin reductase has become the target of choice in gold drug design. Cancerous cells up-regulate the enzymes of the thioredoxin system. This up-regulation may endow selectivity for malignant over normal cells. Gold complexes are the most potent inhibitors of human thioredoxin reductase yet known.[55,68,71]

Mammalian thioredoxin reductase enzymes are homodimeric pyridine disulfide oxidoreductases.[72–75] They catalyze the NADPH-dependent reduction of a disulfide bond in thioredoxin. In so doing, these enzymes preserve the redox balance of the cell. Each subunit of thioredoxin reductase has two electroactive sites: a cysteine-cysteine pair adjacent to FAD, and a cysteine-selenocysteine pair near the *C*-terminus. IC_{50} values for SeCys→Cys mutants implicate selenocysteine as the site of gold binding. Notably, oxidized thioredoxin reductase is uninhibited by gold; the enzyme must be reduced.

Described here are gold(I) complexes with a three-part structure that inhibit mitochondrial thioredoxin reductase. Figure 2 illustrates the general design. Gold attaches to the sulfur atom of 6-mercaptopurine

(6-MP) (Figure 1). Due to its ability to induce apoptosis in B- and T-cells, 6-MP is cytotoxic against acute lymphoblastic leukemia. In addition, the activity of 6-MP against T-cells provides anti-inflammatory properties which are used to treat rheumatoid arthritis.[76] Metabolism of 6-MP leads to the nucleoside triphosphate. This then substitutes for guanine in RNA and DNA synthesis. Once incorporated, 6-MP inhibits chain elongation, and with it, the *de novo* synthesis of purines and cell death results.

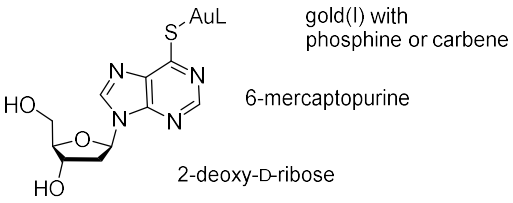

Figure 2. Design of a non-natural nucleoside bearing gold(I).

The design concept unites the enzyme-targeting capacity of gold with the activity of a purine antimetabolite. This work describes the synthesis, chemical characterization, and cytotoxicity of a family of gold(I) 6-mercaptopurinates. The new compounds inhibit rat liver thioredoxin reductase and are toxic toward hyperproliferative cell lines. The pendant sugar moiety solubilizes the complexes in water. Potentially these sugars facilitate transport into the cell.

2. RESULTS AND DISCUSSION

2.1 Synthesis and Characterization. Syntheses of the target nucleosides **8a**–**8c** appear in Scheme 1. The preparation of chloro Hoffer sugar **4** proceeded according to Fieser and Fieser,[77] except that an equivalent amount of hydrochloric acid was used in place of hydrogen chloride gas generated *in situ.* The resulting mixture of the methylfuranoside anomers **2** was acylated by treatment with *p*-toluoyl chloride in pyridine to give **3**. Compound **3** was converted to **4** with a solution of HCl in acetic acid prepared as follows: HCl was generated *in situ* by adding 16.3 mL acetyl chloride to a solution of 81 mL acetic acid and 4 mL water. The sodium salt of commercially available 6-chloropurine, generated *in situ* by the treatment of sodium hydride and 6-chloropurine in acetonitrile, was reacted with 1-chloro-2-deoxy-3,5-di-*O*-*p*-toluoyl-α-d-erythro-pentafuranose (**4**) at ambient temperature under nitrogen. An isomeric mixture of nucleosides formed, where sugars bind at positions N-7 and N-9 of 6-mercaptopurine. After silica gel column chromatography (as detailed in the experimental section), the N-9 isomer, 6-chloro-9-(2-*deoxy*-3,5-di-*O*-*p*-toluoyl-*β*-D-*erythro*-pentofuranosyl)purine (**5**) was isolated in 60% yield, while 20% of N-7 glycosyl isomer was collected as well. No α-anomer was detected by TLC, in agreement with the literature.[78] When **5** was treated with 2 equiv of NaSH in methanol, nucleophilic displacement of chlorine gave 9-(2-deoxy-3,5-di-*O*-*p*-toluoyl-*β*-d-*erythro*-pentofuranosyl)purine-6-thione (**6**).

Deprotection of the carbohydrate proceeded by treating **6** with methanolic ammonia to isolate **7** at 73% yield. Compound **7** was then reacted with Ph_3PAuCl and excess base to yield **8a**. The characteristic $^{31}P\{^1H\}$ resonance shifts 2.5 ppm downfield in **8a** relative to that of Ph_3PAuCl, δ 34.1 ppm. An apparent triplet resonance at δ 6.3–6.5 ppm (J = ~7 Hz), assignable to the hydrogen attached to the glycosidic carbon, is characteristic of the β-anomer of complexes **8a–c**.[20]

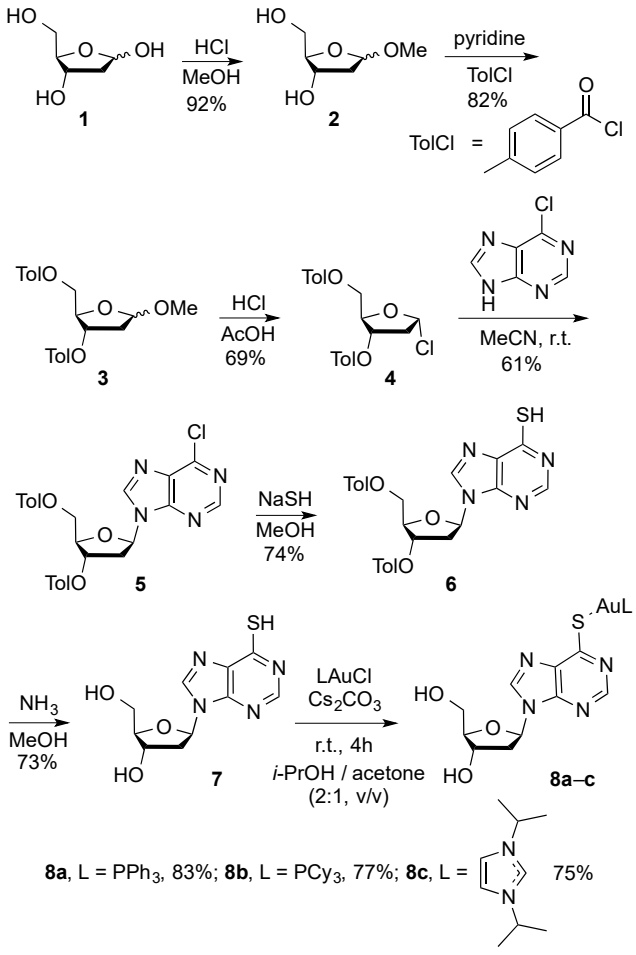

Scheme 1. Synthesis of gold containing nucleosides

The final compounds were purified by silica-gel column chromatography (diethyl ether and methanol 4:1, v/v) and recrystallized from hot methanol.

2.2 X-ray Crystallography. Vapor diffusion of diethyl ether into a concentrated THF solution yielded diffraction-quality crystals of **8b**. The structure appears in Figure 3. The complex crystallizes in the monoclinic space group $P2_1$. Two crystallographically independent copies of **8b** and two THF molecules of crystallization occupy the asymmetric unit. Metric parameters appear in the figure caption. The structures of the tricyclohexylphosphine ligand, the nucleobase, and the sugar are unexceptional. The bond angle S1–Au1–P1 is 179.16(7)° in keeping with the near-linear geometry of most gold(I) complexes.[79–82] The Au1–S1 distance is 2.3095(19) Å and Au1–P1 bond distance is 2.2719(18); both are normal.

2.3 Cellular Effects of 8a. The cytotoxicity of **8a** was evaluated against four human cancer cell lines: Leukemia (MOLT 4 and CCRF CEM-7), breast (MCF-7) and cervical (HeLa) cancer. As a positive control, experiments were also performed examining the cytotoxic effects of the free ligand **7** and Ph_3PAuCl against these leukemia and adherent cell lines.

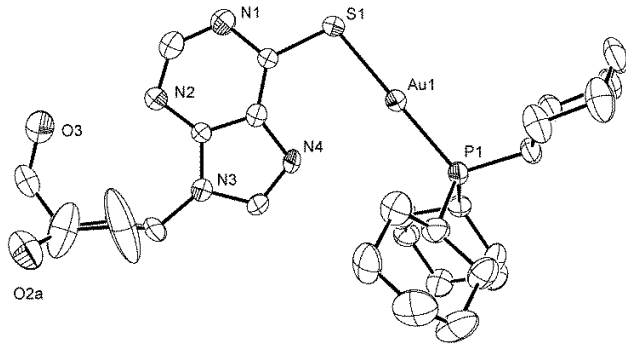

Figure 3. Crystal structure of one independent molecule of **8b**. Thermal ellipsoids are shown at 50% probability; hydrogen atoms are omitted for clarity. A partial atom labelling scheme appears; unlabeled atoms are carbon.

The cytotoxicity of **8a** was quantified by measuring cell viability as a function of drug-concentration using the Presto Blue cell viability assay (please see experimental section for details).[83] Cells were exposed to concentrations of **8a** ranging from 0.001–100 µM for time periods of up to 72 h before cell viability was assessed. In all cases, total cell count and cell viability decrease as the concentration of **7** or **8a** increases. A fit of the data to equation 1,

$$Y = \frac{100\%}{1 + \frac{IC_{50}}{[\text{Inhibitor}]}}, \qquad (1)$$

provides IC_{50} values of 17.9 ± 1.5 µM (**7**) and 0.030 ± 0.008 µM (**8a**) against CCRF CEM-7 cells.

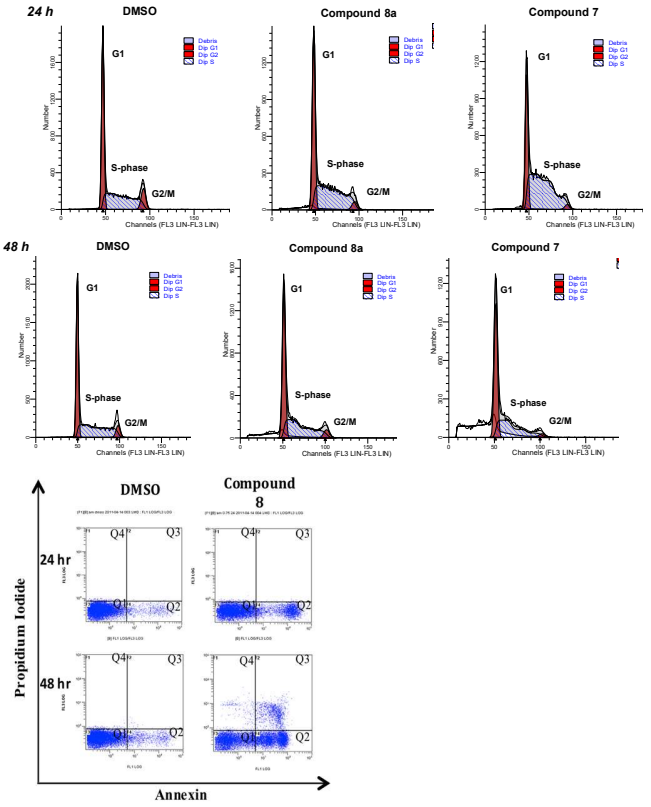

Figure 4. Cell cycle analyses of MOLT 4 cells treated with DMSO, 0.6 µM of compound **8a**, and 12 µM compound **7.** (Upper) Annexin-PI staining of MOLT 4 cells treated with compound **8a** for 48 hr. (Lower)

Table 1. Summary of LD_{50} and IC_{50} values for compounds **7**, **8a,** and Ph_3PAuCl against selected adherent and systemic cancer cell lines.[a]

		7	Ph_3PAuCl	**8a**
MOLT 4[b]	LD_{50} (μM)	11.3 ±0.82	1.92 ±0.06	0.59 ± 0.07
	IC_{50} (μM)	6.2 ± 0.1	0.71 ± 0.07	0.30 ± 0.02
CCRF CEM-7[b]	LD_{50} (μM)	27 ± 2	0.15 ± 0.04	0.06 ± 0.008
	IC_{50} (μM)	17.9 ± 1.5	0.05± 0.003	0.03± 0.008
MCF-7[b]	IC_{50} (μM)	>500	11.4 ± 0.8	6.34 ± 0.55
HeLa[b]	IC_{50} (μM)	>500	6.5 ± 0.5	1.65 ± 0.04

[a] Assays were performed as described in experimental section. LD_{50} is the concentration of drug that reduces cell viability to 50% of that of untreated control cells. IC_{50} is the concentration of the drug that inhibits cell growth to 50% of that of untreated control cells. [b] MOLT 4, CCRF CEM-7 = human acute lymphoblastic leukemia cell lines, MCF-7 = human breast adenocarcinoma cell line, HeLa = human

Table 1 summarizes LD_{50} and IC_{50} values for **8a** against the four cell lines. Compound **8a** displays cytotoxic effects against all tested cell lines, with LD_{50} values ranging from nM to μM. Comparison of the LD_{50} values indicates that **8a** is more effective against systemic (leukemia) cell lines than adherent cell lines. The highest potency occurs against CCRF CEM-7 cells for which IC_{50} = 30 nM and LD_{50} = 60 nM. In all cases, the inclusion of the gold pharmacophore increases the potency of 7. For example, the LD_{50} of **7** is 19-fold higher compared to **8a** against MOLT 4 cells (compare 11.3 ± 0.8 μM for **7** and 0.59 ± 0.07 μM for **8a**). More dramatic effects are observed against CCRF CEM-7 cells as the potency of **7** is 400-fold lower than that of **8a** (compare 27 ± 2 μM for **7** and 0.06 ± 0.008 μM for **8a**). The IC_{50} values for **8a** against adherent cell lines are in the micromolar range (MCF-7, 6.34 ± 0.55 μM; HeLa, 1.65 ± 0.04 μM), while free nucleoside **7** does not show cytotoxicity when tested up to 500 μM concentration. Collectively, these data indicate that the potency of compound **7** is increased significantly upon the inclusion of the Au(I) triphenylphosphine moiety.

Results of control experiments using Ph_3PAuCl are summarized in Table 1. Replacing the chloride ligand with **7** augments the potency of the aggregate. In particular, the potency nearly doubles in the case of CCRF CEM-7 (Ph_3PAuCl, 0.15 ± 0.04 μM; compound **8a**, 0.060 ± 0.008 μM) and MCF-7 cell line (Ph_3PAuCl, 11.4 ± 0.82 μM; compound **8a**, 6.3 ± 0.6 μM) while the same effect is observed in the case of MOLT 4 (Ph_3PAuCl, 1.92 ± 0.06 μM; compound **8a**, 0.59 ± 0.07 μM) and HeLa (Ph_3PAuCl, 6.5 ± 0.5 μM; compound **8a**, 1.65 ± 0.04 μM) cells.

2.4 Mechanism of cell death in leukemia cells. The cellular mechanism by which **8a** causes cell death in MOLT 4 cells was evaluated employing dual parameter fluorescence-activated cell sorting (FACS) analyses to measure propidium iodide (PI) uptake coupled with Alexa Fluor 488 annexin V conjugate staining. In this analysis, live cells (negative for either fluorophore) are easily distinguished from cells that are early apoptotic (annexin V positive and PI negative), late apoptotic (PI and annexin V positive), or necrotic (PI positive and annexin V negative). In these experiments, MOLT 4 cells were treated with 1 μM **8a** for 24 and 48 h, respectively, and then analyzed using dual annexin/propidium iodide staining. Results provided in Figure 4, show a significant accumulation of early apoptotic cells after treated with **8a** for 24 h compared to DMSO. After 48 hours of treatment with **8a**, there is a significant accumulation of both early and late apoptotic cells compared to cells treated with DMSO. This result concurs with experiments measuring cellular viability described earlier that demonstrate a dose- and time-dependent effect of **8a** on cell viability.

Cell-cycle analyses were next performed to determine if **8a** affects DNA synthesis in highly proliferative MOLT 4 cancer cells. FACS analysis using propidium iodide (PI) staining was performed to assess the DNA content of the cells after 24 h of drug treatment. Cells were treated with LD_{50} concentrations of **8a** while IC_{50} concentrations of **7** were used as positive control. Cells were also treated with DMSO as a negative control. Representative data for cell treated with these various agents are provided in Figure 4. After 24 h of treatment with **8a**, the percentage of cells in S-phase increased from 44.9 ± 0.1% (DMSO control) to 54.5 ± 0.1% for **8a**. However this S-phase block is not as pronounced as that for treatment with **7** (68.2 ± 0.1%), which is a known anti-leukemic agent. This result is notable since the concentration of **8a** used in this experiment is 20 times lower than that of **7**. It is well established that **7** functions as an anti-metabolite that can interfere with nucleotide metabolism. This interference causes reduction in dNTP pools which then indirectly inhibits DNA synthesis and causes an accumu-

lation of cells at S-phase. The data presented here suggests that **8a** may function similarly to **7** but with higher potency. However, **8a** may also alter the activity of other cellular targets associated with cell-cycle progression as similar effects on cell-cycle progression were observed using different (phosphine)Au(I)−indole compounds.[84] Possible targets for **8a** include kinases involved in the transition from S-phase to G2/M.

2.5 Mechanism of cell death in adherent cancer cells. Cell-cycle analyses were also performed against an adherent cancer cell line, MCF-7, to determine if **8a** affects DNA synthesis similarly compared to systemic cancer cells such as MOLT 4. Again, FACS analysis with propidium iodide (PI) staining was used to assess DNA content in adherent cells treated with **8a** for 24 and 48 hr, respectively (data not shown). Cells were also treated with DMSO as a negative control. In this case, there is an accumulation of subG1 DNA in cells treated with **8a** compared to cells treated with DMSO. This increase in subG1 DNA is consistent with the induction of apoptosis. In addition, there is a time-dependent increase in the amount of subG1 DNA as well as a concentration dependency. These results again indicate that **8a** produces anti-cancer effects against adherent cancer cell lines, albeit with reduced potency compared to haematological cancer cells.

To further interrogate the cellular basis for this apparent apoptotic effect, we next measured mitochondrial viability of cells treated with **8a** versus DMSO. Collapse of the mitochondrial membrane potential is a biochemical event associated with early-stage apoptosis. Membrane potential loss was detected by microscopy using the cationic fluorescent dye JC-1 as a biomarker for mitochondrial integrity. Aggregates of JC-1 emit red, whereas the monomer shows green luminescence. HeLa cells were treated with 7 μM **8a** or with DMSO (vehicle) for 48 h, and the results are presented in Figure 5. As indicated, cells treated with DMSO take up JC-1 which then accumulates in the mitochondria and produces the red dots seen in Figure 5(a). Cells exposed to **8a** change shape without showing mitochondrial uptake of JC-1. Rather, the dye disperses throughout the cytoplasm and the cell appears green (Figure 5(b)).

2.6 Inhibition of Thioredoxin Reductase. The inhibitory potential of **8a** toward rat liver thioredoxin reductase (TrxR) was evaluated using a standard dithionitrobenzoate (DTNB) reduction assay.[85] TrxR reduces the disulfide bond of DTNB leading to the formation of 5-thionitrobenzoic acid which is detected photometrically (λ_{max} = 412 nm). Figure 6 plots the time course for the absorbance changes associated with conversion of DTNB to 5-thionitrobenzoic acid in the absence and presence of different concentrations of **8a**. In the absence of **8a**, TrxR shows a rapid rate of converting DTNB to 5-thionitrobenzoic acid, and this rate represents 100% activity. The addition of 0.1 μM **8a** inhibits TrxR activity by 33% while the addition of 1 μM **8a** inhibits TrxR activity by greater than 90%. These data suggest that TrxR is a possible target for **8a** and could account for its anti-cancer activity. However, other cellular targets such as kinases and ribonucleotide reductase are plausible targets as well.

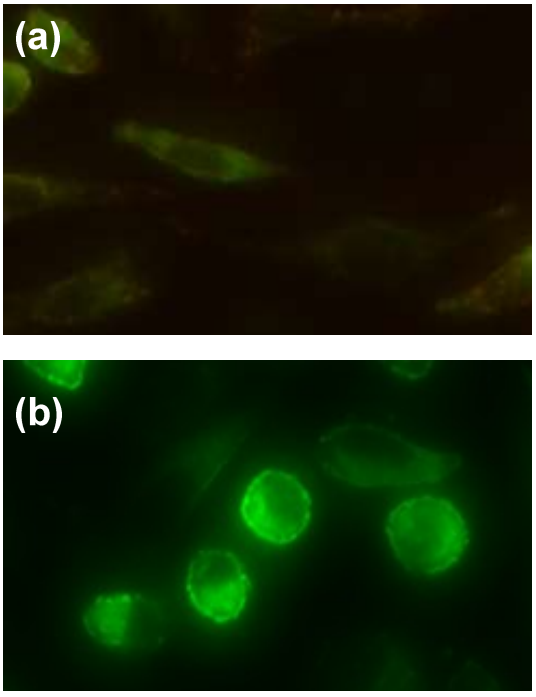

Figure 5. (a) MOLT 4 cells incubated in DMSO vehicle (control) 48 h. (b) Cells after 48 h incubated with 7 μM **8a**.

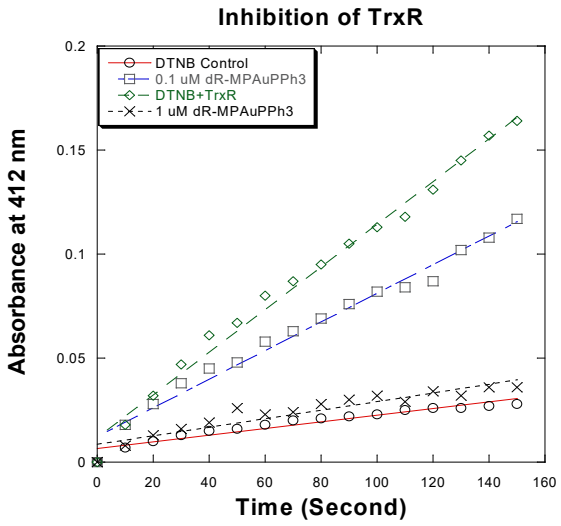

Figure 6. Thioredoxin reductase inhibition assay: Intensity of DTNB absorption *vs.* time. Linear least-squares fits are indicated.

3. CONCLUSIONS

We describe syntheses of non-natural nucleosides bearing (6-mercaptopurinato)gold(I) in the nucleobase position. Terminal ligands on gold are triphenylphosphine (**8a**), tricyclohexylphosphine (**8b**), and an *N*-heterocyclic carbene (**8c**). The new compounds are air- and moisture-stable and do not require extraordinary precautions. Compound **8b** has been crystallographically characterized. The structure shows normal two-coordination at gold. The Cy_3PAu fragment binds to the mercaptopurine sulphur. Close approaches to other potential electron donors are not found, and aurophilic Au···Au interactions are absent.

Compound **8a** was evaluated against a panel of four malignant cell lines. Potency was greatest against CCRF CEM-7 cells, for which IC_{50} = 30 nM and LD_{50} = 60 nM. Compound **8a** induces apoptosis in MOLT 4 cells. A mitochondrial permeability transition assay and thioredoxin reductase activity assay combine to suggest TrxR as a possible target.

4. EXPERIMENTAL SECTION

Reagents and General Methods. Experimental procedures involving air- or moisture sensitive substances were performed under argon using Schlenk line techniques or in a nitrogen-filled MBraun drybox. Anhydrous solvents were used directly from an MBraun solvent purification system or were purchased from Sigma-Aldrich. NMR spectra (^{1}H and ^{31}P{^{1}H}) were recorded on a Varian AS-400 spectrometer operating at 399.7 and 161.8 MHz, respectively. Chemical shifts are reported in parts per million (δ), measured from tetramethylsilane (0 ppm) and are referenced to the solvent $CDCl_3$ (7.26 ppm) or MeOH-d_4 (3.31 ppm) for ^{1}H NMR. For ^{31}P{1H} NMR spectra, chemicals shifts were determined relative to 85% aqueous H_3PO_4. High-resolution electrospray ionization mass spectrometry (Hi-Res ESI-MS) experiments were performed on an IonSpec HiRes ESI-FTICRMS at the University of Cincinnati Mass Spectrometry facility. Thin layer chromatography (TLC) was carried out using Whatman Silica Gel UV254 plates. Column chromatography was performed using Fisher Scientific Silica Gel, sizes 32–63. Elemental analyses were carried out by Robertson Microlit Laboratories, Ledgewood, NJ.

All chemicals were purchased from Sigma-Aldrich or Acros as highest purity grade and used without further purification. 6-chloropurine and sodium hydrogen sulfide were purchased from Sigma-Aldrich. 2-Deoxy-d-ribose, pyridine, *p*-toluoyl chloride and acetyl chloride were purchased from Acros Organics. Bovine serum albumin was obtained from Sigma-Aldrich. Presto-Blue reagent, apoptosis Kit #2, and thioredoxin reductase were purchased from Invitrogen. Cell-titer blue reagent was purchased from Promega. Purity of all biologically active compounds was >95% as judged by micro-combustion analyses (C, H, and N) performed by Robertson Microlit Laboratories (Ledgewood, NJ).

Ph_3PAuCl was synthesized by a slight modification of the literature procedures (using toluene and Au(THT)Cl).[30] Similarly compound **4** was synthesized according to a published procedure.[31]

6-Chloro-9-(2-*deoxy*-3,5-di-*O*-*p*-toluoyl-*β*-d-*erythro*-pentofuranosyl)purine, (5). A mixture of 6-chloropurine (1.790 g, 11.581 mmol) and anhydrous sodium hydride (0.305 g, 12.74 mmol) in anhydrous acetonitrile (80 mL) was stirred at ambient temperature for 30 minutes inside a glove box. Dry, powdered 1-chloro-2-deoxy-3,5-di-*O*-*p*-toluoyl-α-D-*erythro*-pentafuranose, **4** (4.954 g, 12.74 mmol) was added by portions over a period of 20 minutes and stirring was continued for a further 18 hours at rt. After completion of the reaction, any small amount of insoluble

material present in the mixture was removed by filtration. Evaporation of the solvent resulted in an oily residue, which was further purified by silica gel column chromatography. The desired N-9 isomer was isolated as the first major fraction by eluting a mixture of hexanes and diethyl ether (3:2, v/v). Evaporation of the solvent under reduced pressure and drying under vacuum for 4 h yielded analytically pure product as white solid. Yield: 3.58 g, 61%. ^{1}H NMR (400 MHz, $CDCl_3$), δ: 8.67 (s, 1H), 8.29 (s, 1H), 7.97 (d, 2H, *J* = 8.0 Hz), 7.86 (d, 2H, *J* = 8.4 Hz), 7.29 (d, 2H, *J* = 8.8 Hz), 7.21 (d, 2H, *J* = 8 Hz), 6.57 (t_{app}, 1H, *J* = 5.6 Hz), 5.84–5.82 (m, 1H), 4.80 (d, 1H, *J* = 10 Hz), 4.68–4.63 (m, 2H), 3.17–3.13 (m, 1H), 2.92–2.89 (m, 1H), 2.44 (s, 3H), 2.40 (s, 3H). HRMS: Calcd. for $C_{26}H_{24}ClN_4O_5$ $[M+H]^+$: 507.1435 Found: 507.1423. Anal. Calcd. for $C_{26}H_{23}ClN_4O_5$: C, 61.60; H, 4.57; N, 11.05. Found: C, 61.86; H, 4.81; N, 11.34.

9-(2-*deoxy*-3,5-di-*O*-*p*-toluoyl-*β*-d-*erythro*-pentofuranosyl)purine-6-thione, (6). Compound **5** (1.210 g, 2.390 mmol) was suspended in 40 mL anhydrous methanol with continuous stirring under argon. To this was added a solution of NaSH (0.268 g, 4.781 mmol) in 10 mL anhydrous methanol. The reaction mixture was stirred at rt for 8 h. Solvent was removed under vacuum and the resulting yellow residue was purified by silica gel column chromatography. The product was collected by eluting a solvent mixture of diethyl ether and methanol (9:1, v/v). Yield: 0.892 g, 74 %. ^{1}H NMR (400 MHz, $CDCl_3$), δ: 8.24 (s, 1H), 8.11 (s, 1H), 7.94 (d, 2H, *J* = 8.1 Hz), 7.87 (d, 2H, *J* = 7.9 Hz), 7.26 (d, 2H, *J* = 7.7 Hz), 7.21 (d, 2H, *J* = 7.8 Hz), 6.45 (t_{app}, 1H, *J* = 7.1 Hz), 5.78 (d, 1H, *J* = 6.7 Hz), 4.76–4.71 (m, 1H), 4.67–4.61 (m, 2H), 3.10–3.02 (m, 1H), 2.80 (ddd, 1H, *J* = 14.4, 6.4, 2.1 Hz), 2.42 (s, 3H), 2.38 (s, 3H). HRMS: Calcd. for $C_{26}H_{24}N_4NaO_5S$ $[M+Na]^+$: 527.1365 Found: 527.1361. Anal. Calcd. for $C_{26}H_{24}N_4O_5S$: C, 61.89; H, 4.79; N, 11.10. Found: C, 62.21; H, 4.67; N, 10.82.

9-(2-deoxy-*β*-d-*erythro*-pentofuranosyl)purine-6-thione (7). A solution of **6** (0.850, 1.684 mmol) in methanolic ammonia (saturated by passing ammonia gas for 15 min at 0 °C, 40 mL) was allowed to stir at room temperature for 20 h. After that, the solvent was evaporated under reduced pressure to dryness, and the residue was purified by column chromatography using silica gel. The desired product was collected as the major fraction when eluted with a mixture of diethyl ether and methanol (4:1, v/v). Solvent was removed under reduced pressure, and the desired product was collected as white powder. Yield: 0.330 g, 73%. ^{1}H NMR (400 MHz, CD_3OD), δ: 8.44 (s, 1H), 8.12 (s, 1H), 6.43 (t_{app}, 1H, *J* = 7.0 Hz), 4.54 (m, 1H), 4.02 (q, 1H, *J* = 3.5 Hz), 3.75 (ddd, 2H, *J* = 15.2, 11.6, 3.5 Hz), 2.70 (quin, 1H, *J* = 7.5 Hz), 2.46 (m, 1H). HRMS: Calcd. for $C_{10}H_{13}N_4O_3S$ $[M+H]^+$: 269.0708 Found: 269.0704. Anal. Calcd. for $C_{10}H_{12}N_4O_3S$: C, 44.77; H, 4.51; N, 20.88. Found: C, 44.86; H, 4.73; N, 20.83.

(9-(2-deoxy-*β*-D-*erythro*-pentofuranosyl)purine-6-thio)(triphenylphosphine)gold(I) (8a). Compound **7** (0.070 g, 0.261 mmol) and Cs_2CO_3 (0.170 g, 0.522 mmol) were suspended in 2-propanol (20 mL) under argon. A solution of Ph_3PAuCl (0.130 g, 0.261 mmol) in 10 mL dry acetone was added dropwise into the stirred mixture. The reaction flask was sealed, and the mixture was stirred room temperature for 4 h. After this time, the solvent was removed under reduced pressure. The white residue was purified on a small silica gel column by eluting a mixture of diethyl ether and methanol (4:1, v/v). The desired product was collected as major fraction. Removal of solvent and drying in vacuum for 6 h gave analytically pure product. Yield: 0.157 g, 83 %. ^{1}H NMR (400 Hz, CD_3OD), δ: 8.39 (s, 1H), 8.31 (s, 1H), 7.68–7.63 (m, 6H), 7.58–7.50 (m, 9H), 6.45 (t_{app}, 1H, *J* = 6.5 Hz), 4.58 (q, 1H, *J* = 2.7 Hz), 4.06–4.04 (m, 1H), 3.79 (ddd, 2H, *J* = 17.2, 5.4, 3.6 Hz), 2.83–2.77 (m, 1H), 2.46 (ddd , 1H, *J* = 13.3, 5.9, 3.1 Hz). ^{31}P{^{1}H} NMR (CD_3OD), δ: 37.5. HRMS: Calcd. for $C_{28}H_{27}AuN_4O_3PS$ $[M+H]^+$: 727.1207 Found: 727.1228. Anal. Calcd. for $C_{28}H_{26}AuN_4O_3PS$: C, 46.29; H, 3.61; N, 7.71. Found: C, 46.51; H, 3.93; N, 8.03.

(9-(2-deoxy-*β*-D-*erythro*-pentofuranosyl)purine-6-thio)(tricyclohexylphosphine)gold(I) (8b). Compound **7** (0.070 g, 0.261 mmol) and Cs_2CO_3 (0.170 g, 0.522 mmol) were suspended in 2-propanol (20 mL) under argon. A solution of Cy_3PAuCl (0.134 g, 0.261 mmol) in 10 mL dry acetone was added dropwise to the stirred mixture. The reaction flask was sealed and stirred at room temperature for 4 h. After completion of the reaction, the solvent was removed under reduced pressure. The white residue was purified on a small silica gel column by eluting a mixture of diethyl ether and methanol (4:1, v/v). The desired product was collected as the major fraction. Evaporation of solvent under reduced pressure and drying in vacuum for 6 h gave analytically pure product. Yield: 0.150 g, 77%. ^{1}H NMR (400 Hz, $CDCl_3$), δ: 8.42 (s, 1H), 7.83 (s,

1H), 6.33 (t_{app}, 1H, *J* = 6.5 Hz), 4.11 (q, 1H, *J* = 7.2 Hz), 3.98–3.77 (m, 2H), 3.10–3.03 (m, 1H), 2.83–2.77 (m, 1H), 2.30 (dd , 1H, *J* = 13.7, 5.3 Hz), 2.07–2.03 (m, 6H), 1.87–1.84 (m, 6H), 1.74–1.72 (m, 3H), 1.56–1.53 (m, 6H), 1.35–1.22 (m, 12H). $^{31}P\{^{1}H\}$ NMR ($CDCl_3$), δ: 57.6. HRMS: Calcd. for $C_{28}H_{45}AuN_4O_3PS$ $[M+H]^+$: 745.2616 Found: 745.2603. Anal. Calcd. for $C_{28}H_{44}AuN_4O_3PS$: C, 45.16; H, 5.96; N, 7.52. Found: C, 45.27; H, 5.77; N, 7.27.

(9-(2-deoxy-*β*-D-*erythro*-pentofuranosyl)purine-6-thio)(1,3-diisopropylimidazol-2-ylidene)gold(I) (8c). Compound **7** (0.070 g, 0.261 mmol) and Cs_2CO_3 (0.170 g, 0.522 mmol) were suspended in 2-propanol (20 mL) under argon. A solution of (1,3-diisopropylimidazol-2-ylidene)gold(I) chloride (0.101 g, 0.261 mmol) in 10 mL dry acetone was added dropwise into the stirred mixture. The reaction flask was sealed, and stirring continued at room temperature for 4 h. Solvent was then removed under reduced pressure. The white residue was purified passage through silica, eluting with a mixture of diethyl ether and methanol (4:1, v/v). The desired product was collected as the major fraction. Removal of solvent and drying in vacuum for 6 h gave analytically pure product. Yield: 0.121 g, 75%. ^{1}H NMR (400 Hz, CD_3OD), δ: 8.43 (s, 1H), 8.35 (s, 1H), 7.40 (s, 2H), 6.46 (t_{app}, 1H, *J* = 6.9 Hz), 5.26 (sep, 2H, *J* = 7.1 Hz), 4.59 (m, 1H), 4.07–4.05 (m, 1H), 3.87–3.71 (m, 2H), 2.86–2.79 (m, 1H), 2.46 (ddd, 1H, *J* = 12.6, 6.2, 2.9 Hz), 1.53 (d, 12H, *J* = 7.2 Hz). HRMS: Calcd. for $C_{19}H_{28}AuN_6O_3S$ $[M+H]^+$: 617.1609 Found: 617.1691. Anal. Calcd. for $C_{19}H_{27}AuN_6O_3S$: C, 36.96; H, 4.57; N, 13.61. Found: C, 37.30; H, 4.79; N, 13.82.

General Cell Culture Procedures. HeLa, MCF-7, MOLT 4 and CEM-C7, were obtained from the American Type Culture Collection (Manassas, VA, USA). All adherent cell lines were maintained in Dulbecco's modified Eagle's medium (Mediatech) with 100 U/mL penicillin (Invitrogen), 100 µg/mL streptomycin (Invitrogen), 0.25 µg/mL amphotericin B (Invitrogen), and 10% fetal bovine serum(USA Scientific) and incubated at 37 °C with 5% CO_2. CEM and MOLT 4 cells were maintained in RPMI-1640 media supplemented with 100 U/mL penicillin, 100 µg/mL streptomycin, 0.25 µg/mL amphotericin B, and 10% fetal bovine serum and incubated at 37 °C with 5% CO_2. Compounds were freshly dissolved as stock solutions in DMSO prior to the experiments. Unless stated otherwise, the final concentration of the DMSO vehicle was 0.1% (v/v).

Cell Proliferation Assays. Cells were plated at a density of 7,000-13,000/well in 200 µL of media overnight in a 96-well plate. Each drug was added to wells in a dose-dependent manner (0.01-100 µM). Cells were treated with compounds for variable time periods (8-48 hours). With adherent cell lines, medium was removed from the wells and then 90 µL of fresh medium was added into each well followed by the addition of 10µL of PrestoBlue Cell Viability Reagent (invitrogen). Cells were incubated with reagent for 20-60 minutes and the optical density of samples was read at 595 nm using a microplate reader. The background absorbance of dye with media was subtracted from each sample. Cell viability was then normalized against cells treated with DMSO. IC_{50} values were obtained using a fit of the data to Equation 1.

Measurements of Apoptosis. Cells were plated at 250,000/mL, different analogues were added in a dose-dependent fashion for 12-48 hr. Cells were trypsinized and then washed with cold PBS. After discarding the supernatant, a 100 µL solution containing 1X annexin-binding buffer, 5 µL of Alexa Fluor 488 Annexin V and 1 µg/mg of PI solution was added to each sample. The cells were incubated at room temperature for 15 min. After this incubation period, an additional 400 µL of 1X annexin-binding buffer was added. Cells were analyzed using band pass filters with wavelengths of 525/40 nm and 620/30 nm with a Beckman Coulter XL flow cytometer.

Cell Cycle Analyses. Cells were plated at a density of 200,000/mL. The compounds were then added in a dose-dependent manner for time periods varying from 1 to 3 days. Cells were treated with 0.25% trypsin and harvested by centrifugation. The supernatant was removed and then washed with PBS. After aspiration of PBS, 500 µL of 70% ethanol was added and cells were incubated on ice for 15 minutes followed by centrifugation and the removal of ethanol. One mg of PI staining solution [(10 mg of 0.1 Triton X-100/PBS, 0.4 mg of 500 µg/mL of PI, and 2 mg/mg of DNase-free RNase)] was added to the cell suspension, placed on ice for 30 minutes, and then analyzed using a Beckman Coulter XL flow cytometer with a red filter. Analysis was performed by ModFit software.

Assessment of the Mitochondrial Membrane Potential. Cells were cultured on 12 well plate at a cell density optimal for apoptosis induction and minimizing any cell sloughing. After incubation of 24-48 hours with different concentrations of compound **8**, around

1-2 million of suspension cells were centrifuged and washed with PBS. For adherent cell lines cells are plated at density of 2000/mL in a 12 well plate. After 48 hours of drug treatment, the supernatant was removed. The cells are then suspended with 0.5 mL1X MitoPT JC-1 solution (MitoPT™-JC1 Assay Kit, Immuno Chemistry Technologies, LLC). The cells were incubated for 20 minutes at 37 °C. Control cells were likewise incubated with JC1 dye. The suspension cells were centrifuged and washed several times with the assay buffer. A monolayer of cells was formed and covered with a sterile cover slip. In case of adherent cells the monolayer was washed with 1-2 mL of assay buffer and one drop of assay buffer was placed and covered with a sterile cover slip. The integrity of cells was assessed by an optical microscope.

Thioredoxin Reductase Inhibition. Commercially available rat liver TrxR (Sigma) was used to determine the inhibitory effect of the gold drugs towards TrxR. The assay was performed following the manufacturer's instructions (Sigma product information sheet T 9698). Before each experiment 10 µL of supplied rat liver TrxR was diluted to give 100 µL TrxR solution in potassium phosphate buffer. 10 µL of this aliquot (containing approximately 0.06 unit of TrxR) was placed in a 0.5 mL cuvette along with 10 µL of the required gold drug with increasing concentration, 80 µL distilled water and 500 µL reaction mixture (10 mg of reaction mixture consisted of 1.0 mg of 1.0 M potassium phosphate buffer, pH 7.0, 0.20 mg of 500 mM EDTA solution pH 7.5, 0.80 mg of 63 mM DTNB in ethanol, 0.10 mg of 20 mg/mL bovine serum albumin, 0.05 mg of 48 mM NADPH and 7.85 mg of water). After mixing properly the formation of 5-thionitrobenzol was monitored by measuring the absorbance at 412 nm using BioRad SmartSpec™ 3000 spectrophotometer over 3 min in 10 s intervals. The increase in 5-thionitrobenzol over time followed a linear trend ($r^2 \geq 0.99$), and the enzymatic activities were calculated as the slopes (increase in absorbance per second) thereof.

Acknowledgements

The authors thank the U.S. National Science Foundation (grant CHE-1057659 to T. G. G.) and the Department of Defence, US Army Medical Research (CA091380 to A. J. B.) for support. N. D. thanks the Republic of Turkey for a fellowship.

Notes

Crystallographic data for **8b** were deposited with the Cambridge Crystallographic Data Centre, deposition number CCDC 1015466. These data can be obtained free of charge via www.ccdc.cam.ac.uk/data_request/cif, by e-mailing data_request@ccdc.cam.ac.uk or by contacting The Cambridge Crystallographic Data Centre, 12 Union Road, Cambridge CB2 1EZ, UK; fax: +44(0)1223-336033.

References

1. Sadler, P. J. The biological chemistry of gold: A Metallo-drug and heavy-atom label with variable valency. in Biochemistry 171–214 (Springer Berlin Heidelberg, 1976).

2. Shaw, C. F. Mammalian Biochemistry of gold-inorganic perspective of chrysotherapy. Inorg. Perspect. Biol. Med. 2, 287–355 (1979).

3. Brown, D. H. & Smith, W. E. The chemistry of the gold drugs used in the treatment of rheumatoid arthritis. Chem. Soc. Rev. 9, 217–240 (1980). https://doi.org/10.1039/cs9800900217

4. Elder, R. C. & Eidsness, M. K. Synchrotron x-ray studies of metal-based drugs and metabolites. Chem. Rev. 87, 1027–1046 (1987). https://doi.org/10.1021/cr00081a008

5. Shaw, C. F. I. Gold-Based Therapeutic Agents. Chem. Rev. 99, 2589–2600 (1999). https://doi.org/10.1021/cr980431o

6. Shaw, III., C. F. In Gold: Progress in Chemistry, Biotechnology, and Technology, H. Schmidbaur, Ed. (Wiley, 1999).

7. Tiekink, E. R. T. & Ho, S. Y. Metallotherapeutic Drugs & Metal-based Diagnostic Agents: The Use of Metals in Medicine. (Wiley).

8. Simon, T. M., Kunishima, D. H., Vibert, G. J. & Lorber, A. Inhibitory effects of a new oral gold compound on hela cells. Cancer 44, 1965–1975 (1979). https://doi.org/10.1002/1097-0142(197912)44:6<1965::AID-CNCR2820440602>3.0.CO;2-6

9. Simon, T. M., Kunishima, D. H., Vibert, G. J. & Lorber, A. Screening Trial with the Coordinated Gold

Compound Auranofin Using Mouse Lymphocytic Leukemia P388. Cancer Res. 41, 94–97 (1981). PMid:6778607

10. Mirabelli, C. K. et al. Correlation of the in Vitro Cytotoxic and in Vivo Antitumor Activities of Gold(1) Coordination Complexes. J. Med. Chem. 29, 218–223 (1986).
PMid:3081721

11. Tiekink, E. R. T. Gold compounds in medicine: Potential anti-tumour agents. Gold Bull. 36, 117–124 (2003). https://doi.org/10.1007/BF03215502

12. Simon, T. M., Kunishima, D. H., Vibert, G. J. & Lorber, A. Cellular antiproliferative action exerted by auranofin. J. Rheumatol. Suppl. 5, 91–97 (1979). PMid:226702

13. Berners-Price, S. J. & Filipovska, A. Gold compounds as therapeutic agents for human diseases. Metallomics 3, 863–873 (2011). https://doi.org/10.1039/c1mt00062d
PMid:21755088

14. Hill, D. T. et al. Seleno-Auranofin (Et3PAuSe-tagl): Synthesis, Spectroscopic (EXAFS, 197Au Mössbauer, 31P, 1H, 13C, and 77Se NMR, ESI-MS) Characterization, Biological Activity, and Rapid Serum Albumin-Induced Triethylphosphine Oxide Generation. Inorg. Chem. 49, 7663–7675 (2010). https://doi.org/10.1021/ic902335z
PMid:20704360

15. Baker, M. V. et al. Synthesis and structural characterisation of linear Au(I) N-heterocyclic carbene complexes: New analogues of the Au(I) phosphine drug Auranofin. J. Organomet. Chem. 690, 5625–5635 (2005). https://doi.org/10.1016/j.jorganchem.2005.07.013

16. de Frémont, P., Stevens, E. D., Eelman, M. D., Fogg, D. E. & Nolan, S. P. Synthesis and Characterization of Gold(I) N-Heterocyclic Carbene Complexes Bearing Biologically Compatible Moieties. Organometallics 25, 5824–5828 (2006). https://doi.org/10.1021/om060733d

17. Barnard, P. J., Baker, M. V., Berners-Price, S. J., Skelton, B. W. & White, A. H. Dinuclear gold(I) complexes of bridging bidentate carbene ligands: synthesis, structure and spectroscopic characterisation. Dalton Trans. 1038–1047 (2004). doi:10.1039/B316804B
https://doi.org/10.1039/B316804B

18. Baker, M. V. et al. Cationic linear Au(I) N-heterocyclic carbene complexes: synthesis structure and anti-mitochondrial activity. Dalton. Trans. 3708–3715 (2006)https://doi.org/10.1039/b602560a
PMid:16865184

19. Barnard, P. J., Baker, M. V., Berners-Price, S. J. & Day, D. A. Mitochondrial permeability transition induced by dinuclear gold(I)–carbene complexes: potential new antimitochondrial antitumour agents. J. Inorg. Biochem. 98, 1642–1647 (2004). https://doi.org/10.1016/j.jinorgbio.2004.05.011
PMid:15458827

20. Hickey, J. L. et al. Mitochondria-targeted chemotherapeutics: the rational design of gold(I) N-heterocyclic carbene complexes that are selectively toxic to cancer cells and target protein selenols in preference to thiols. J. Am. Chem. Soc. 130, 12570–1 (2008). https://doi.org/10.1021/ja804027j
PMid:18729360

21. Rubbiani, R. et al. Comparative in Vitro Evaluation of N-Heterocyclic Carbene Gold(I) Complexes of the Benzimidazolylidene Type. J. Med. Chem. 54, 8646–8657 (2011). https://doi.org/10.1021/jm201220n
PMid:22039997

22. Liu, W. et al. NHC Gold Halide Complexes Derived from 4,5-Diarylimidazoles: Synthesis, Structural Analysis, and Pharmacological Investigations as Potential Antitumor Agents. J. Med. Chem. 54, 8605–8615 (2011).https://doi.org/10.1021/jm201156x
PMid:22091836

23. Dickson, P. N., Wehrli, A. & Geier, G. Coordination chemistry of gold(I) with cyanide and 1-methylpyridine-2-thione. Kinetics and thermodynamics of ligand exchange at gold(I) in aqueous solution. Inorg. Chem. 27, 2921–2925 (1988). https://doi.org/10.1021/ic00290a006

24. Berners-Price, S. J. et al. In Vivo Antitumor Activity and in Vitro Cytotoxic Properties of Bis[1,2-bis(diphenylphosphino)ethane]gold(I) Chloride. Cancer Res. 46, 5486–5493 (1986). PMid:3756897

25. Mirabelli, C. K. et al. Antitumor activity of bis(diphenylphosphino)alkanes, their gold(I) coordination complexes, and related compounds. J. Med. Chem.

30, 2181–2190 (1987). https://doi.org/10.1021/jm00395a004 PMid:3681888

26. Berners-Price, S. J. et al. Cytotoxicity and antitumor activity of some tetrahedral bis(diphosphino)gold(I) chelates. J. Med. Chem. 33, 1386–1392 (1990). https://doi.org/10.1021/jm00167a017 PMid:2329559

27. Berners-Price, S. J. & Sadler, P. J. Phosphines and metal phosphine complexes: Relationship of chemistry to anticancer and other biological activity. in Bioinorganic Chemistry 27–102 (Springer Berlin Heidelberg, 1988).

28. Humphreys, A. S. et al. Gold(i) chloride adducts of 1,3-bis(di-2-pyridylphosphino)propane: synthesis structural studies and antitumour activity. Dalton Trans. 4943–4950 (2007). https://doi.org/10.1039/b705008a PMid:17992279

29. Liu, J. J. et al. In vitro antitumour and hepatotoxicity profiles of Au(I) and Ag(I) bidentate pyridyl phosphine complexes and relationships to cellular uptake. J. Inorg. Biochem. 102, 303–310 (2008). https://doi.org/10.1016/j.jinorgbio.2007.09.003 PMid:18029019

30. Rackham, O., Nichols, S. J., Leedman, P. J., Berners-Price, S. J. & Filipovska, A. A gold(I) phosphine complex selectively induces apoptosis in breast cancer cells: implications for anticancer therapeutics targeted to mitochondria. Biochem. Pharmacol. 74, 992–1002 (2007). https://doi.org/10.1016/j.bcp.2007.07.022 PMid:17697672

31. Wetzel, C. et al. Gold(i) complexes of water-soluble diphos-type ligands: Synthesis, anticancer activity, apoptosis and thioredoxin reductase inhibition. Dalton Trans. 40, 9212 (2011). https://doi.org/10.1039/c1dt10368g PMid:21826354

32. Messori, L. et al. Gold(III) Complexes as Potential Antitumor Agents: Solution Chemistry and Cytotoxic Properties of Some Selected Gold(III) Compounds. J. Med. Chem. 43, 3541–3548 (2000). https://doi.org/10.1021/jm990492u PMid:11000008

33. Cinellu, M. a. et al. [Au 2 (phen 2Me) 2 (μ - O) 2](PF 6) 2, a Novel Dinuclear Gold(III) Complex Showing Excellent Antiproliferative Properties. ACS Med. Chem. Lett. 1, 336–339 (2010). https://doi.org/10.1021/ml100097f PMid:24900215 PMCid:PMC4007953

34. Marcon, G. et al. Gold(III) Complexes with Bipyridyl Ligands: Solution Chemistry, Cytotoxicity, and DNA Binding Properties. J. Med. Chem. 45, 1672–1677 (2002). https://doi.org/10.1021/jm010997w PMid:11931621

35. Messori, L. et al. Solution chemistry and cytotoxic properties of novel organogold(III) compounds. Bioorg. Med. Chem. 12, 6039–6043 (2004). https://doi.org/10.1016/j.bmc.2004.09.014 PMid:15519149

36. Coronnello, M. et al. Mechanisms of Cytotoxicity of Selected Organogold(III) Compounds. J. Med. Chem. 48, 6761–6765 (2005). https://doi.org/10.1021/jm050493o PMid:16220992

37. Casini, A. et al. Chemistry, antiproliferative properties, tumor selectivity, and molecular mechanisms of novel gold(III) compounds for cancer treatment: a systematic study. JBIC J. Biol. Inorg. Chem. 14, 1139–1149 (2009). https://doi.org/10.1007/s00775-009-0558-9 PMid:19543922

38. Ronconi, L. et al. Gold Dithiocarbamate Derivatives as Potential Antineoplastic Agents: Design, Spectroscopic Properties, and in Vitro Antitumor Activity. Inorg. Chem. 44, 1867–1881 (2005). https://doi.org/10.1021/ic048260v PMid:15762713

39. Ronconi, L. et al. Gold(III) Dithiocarbamate Derivatives for the Treatment of Cancer: Solution Chemistry, DNA Binding, and Hemolytic Properties. J. Med. Chem. 49, 1648–1657 (2006). https://doi.org/10.1021/jm0509288PMid:16509581

40. Milacic, V. et al. A Novel Anticancer Gold(III) Dithiocarbamate Compound Inhibits the Activity of a Purified 20S Proteasome and 26S Proteasome in Human Breast Cancer Cell Cultures and Xenografts. Cancer Res. 66, 10478–10486 (2006). https://doi.org/10.1158/0008-5472.CAN-06-3017 PMid:17079469

41. Milacic, V. & Dou, Q. P. The tumor proteasome as a novel target for gold(III) complexes: Implications for breast cancer therapy. Coord. Chem. Rev. 253, 1649–1660 (2009). https://doi.org/10.1016/j.ccr.2009.01.032 PMid:20047011 PMCid:PMC2675785

42. Che, C.-M. & Sun, R. W.-Y. Therapeutic applications of gold complexes: lipophilic gold(iii) cations and gold(i) complexes for anti-cancer treatment. Chem. Commun. 47, 9554 (2011). https://doi.org/10.1039/c1cc10860c PMid:21674082

43. Li, C. K.-L., Sun, R. W.-Y., Kui, S. C.-F., Zhu, N. & Che, C.-M. Anticancer Cyclometalated [AuIIIm(CΛNΛC)mL]n+ Compounds: Synthesis and Cytotoxic Properties. Chem. -Eur. J. 12, 5253–5266 (2006). https://doi.org/10.1002/chem.200600117 PMid:16642532

44. Yan, J. J. et al. Cyclometalated gold(iii) complexes with N-heterocyclic carbene ligands as topoisomerase I poisons. Chem. Commun. 46, 3893 (2010). https://doi.org/10.1039/c001216e PMid:20401423

45. Lum, C. T. et al. Gold(III) porphyrin 1a prolongs the survival of melanoma-bearing mice and inhibits angiogenesis. Acta Oncol. 50, 719–726 (2011). https://doi.org/10.3109/0284186X.2010.537693 PMid:21110776

46. Sun, R. W.-Y. et al. Stable Anticancer Gold(III)-Porphyrin Complexes: Effects of Porphyrin Structure. Chem. -Eur. J. 16, 3097–3113 (2010). https://doi.org/10.1002/chem.201090039 https://doi.org/10.1002/chem.200902741 PMid:20162647

47. Che, C.-M. et al. Gold(iii) porphyrins as a new class of anticancer drugs: cytotoxicity, DNA binding and induction of apoptosis in human cervix epitheloid cancer cells. Chem. Commun. 1718 (2003). https://doi.org/10.1039/b303294a

48. Chow, K. H.-M. et al. A Gold(III) Porphyrin Complex with Antitumor Properties Targets the Wnt/ -catenin Pathway. Cancer Res. 70, 329–337 (2010). https://doi.org/10.1158/0008-5472.CAN-09-3324 PMid:19996284

49. Bhabak, K. P., Bhuyan, B. J. & Mugesh, G. Bioinorganic and medicinal chemistry: aspects of gold(i)-protein complexes. Dalton Trans. 40, 2099–2111 (2011). https://doi.org/10.1039/c0dt01057j PMid:21321730

50. Gunatilleke, S. S. & Barrios, A. M. Inhibition of Lysosomal Cysteine Proteases by a Series of Au(I) Complexes: A Detailed Mechanistic Investigation. J. Med. Chem. 49, 3933–3937 (2006). https://doi.org/10.1021/jm060158f PMid:16789749

51. Baici, A., Camus, A. & Marsich, N. Interaction of the human leukocyte proteinases elastase and cathepsin G with gold, silver and copper compounds. Biochem. Pharmacol. 33, 1859–1865 (1984). https://doi.org/10.1016/0006-2952(84)90540-9

52. Weidauer, E. et al. Effects of disease-modifying anti-rheumatic drugs (DMARDs) on the activities of rheumatoid arthritis-associated cathepsins K and S. Biol. Chem. 388, (2007). https://doi.org/10.1515/BC.2007.037

53. Chircorian, A. & Barrios, A. M. Inhibition of lysosomal cysteine proteases by chrysotherapeutic compounds: a possible mechanism for the antiarthritic activity of Au(I). Bioorg. Med. Chem. Lett. 14, 5113–5116 (2004). https://doi.org/10.1016/j.bmcl.2004.07.073 PMid:15380210

54. Deponte, M. et al. Mechanistic Studies on a Novel, Highly Potent Gold-Phosphole Inhibitor of Human Glutathione Reductase. J. Biol. Chem. 280, 20628–20637 (2005). https://doi.org/10.1074/jbc.M412519200 PMid:15792952

55. Urig, S. et al. Undressing of phosphine gold(I) complexes as irreversible inhibitors of human disulfide reductases. Angew. Chem. Int. Ed Engl. 45, 1881–6 (2006). https://doi.org/10.1002/anie.200502756 PMid:16493712

56. Mendes, F. et al. Metal-Based Inhibition of Poly(ADP-ribose) Polymerase − The Guardian Angel of DNA. J. Med. Chem. 54, 2196–2206 (2011).

57. Krishnamurthy, D. et al. Gold(I)-Mediated Inhibition of Protein Tyrosine Phosphatases: A Detailed in Vitro and Cellular Study. J. Med. Chem. 51, 4790–4795 (2008) https://doi.org/10.1021/jm800101w PMid:18605719

58. Baker, M. A. & Tappel, A. L. Effects of ligands on gold inhibition of selenium glutathione peroxidase. Biochem. Pharmacol. 35, 2417–2422 (1986). https://doi.org/10.1016/0006-2952(86)90470-3

59. Chaudiere, J. & L. Tappel, A. Interaction of Gold(I) with the Active Site of Selenium-Glutathione Peroxidase. J. Inorg. Biochem. 20, 313–325 (1984). https://doi.org/10.1016/0162-0134(84)85030-8

60. Roberts, J. R. & Shaw III, C. F. Inhibition of Erythrocyte Selenium-Glutathione Peroxidase by Auranofin Analogues and Metabolites. Biochem. Pharmacol. 55, 1291–1299 (1998). https://doi.org/10.1016/S0006-2952(97)00634-5

61. Flohe, L., Günzler, W. A. & Schock, H. H. Glutathione peroxidase: A selenoenzyme. FEBS Lett. 32, 132–134 (1973). https://doi.org/10.1016/0014-5793(73)80755-0

62. Rotruck, J. T. et al. Selenium: Biochemical Role as a Component of Glutathione Peroxidase. Science 179, 588–590 (1973). https://doi.org/10.1126/science.179.4073.588 PMid:4686466

63. Chu, F. F., Doroshow, J. H. & Esworthy, R. S. Expression, characterization, and tissue distribution of a new cellular selenium-dependent glutathione peroxidase, GSHPx-GI. J. Biol. Chem. 268, 2571–2576 (1993). PMid:8428933

64. Berry, M. J., Banu, L. & Larsen, P. R. Type I iodothyronine deiodinase is a selenocysteine-containing enzyme. Nature 349, 438–440 (1991). https://doi.org/10.1038/349438a0 PMid:1825132

65. Berry, M. J., Kieffer, J. D., Harney, J. W. & Larsen, P. R. Selenocysteine confers the biochemical properties characteristic of the type I iodothyronine deiodinase. J. Biol. Chem. 266, 14155–14158 (1991). PMid:1830583

66. Gabbiani, C. et al. Thioredoxin reductase an emerging target for anticancer metallodrugs. Enzyme inhibition by cytotoxic gold(iii) compounds studied with combined mass spectrometry and biochemical assays. Med. Chem. Commun. 2, 50–54 (2011). https://doi.org/10.1039/C0MD00181C

67. Marzano, C. et al. Inhibition of thioredoxin reductase by auranofin induces apoptosis in cisplatin-resistant human ovarian cancer cells. Free Radic. Biol. Med. 42, 872–81 (2007). https://doi.org/10.1016/j.freeradbiomed.2006.12.021 PMid:17320769

68. Gromer, S., Urig, S. & Becker, K. The thioredoxin system—From science to clinic. Med. Res. Rev. 24, 40–89 (2004)https://doi.org/10.1002/med.10051 PMid:14595672

69. Gromer, S., Arscott, L. D., Williams, C. H., Schirmer, R. H. & Becker, K. Human Placenta Thioredoxin Reductase: Isolation of the selenoenzyme, steady state kinetics, and inhibition by therapeutic gold compounds. J. Biol. Chem. 273, 20096–20101 (1998). https://doi.org/10.1074/jbc.273.32.20096 PMid:9685351

70. Barnard, P. J. & Berners-Price, S. J. Targeting the mitochondrial cell death pathway with gold compounds. Coord. Chem. Rev. 251, 1889–1902 (2007). https://doi.org/10.1016/j.ccr.2007.04.006

71. Yan, K., Lok, C.-N., Bierla, K. & Che, C.-M. Gold(i) complex of N{,}N[prime or minute]-disubstituted cyclic thiourea with in vitro and in vivo anticancer properties-potent tight-binding inhibition of thioredoxin reductase. Chem. Commun. 46, 7691–7693 (2010).https://doi.org/10.1039/c0cc01058h PMid:20623063

72. Sandalova, T., Zhong, L., Lindqvist, Y., Holmgren, A. & Schneider, G. Three-dimensional structure of a mammalian thioredoxin reductase: Implications for mechanism and evolution of a selenocysteine-dependent enzyme. Proc. Natl. Acad. Sci. U. S. A. 98, 9533–9538 (2001). https://doi.org/10.1073/pnas.171178698 PMid:11481439 PMCid:PMC55487

73. Holmgren, A. & Lu, J. Thioredoxin and thioredoxin reductase: Current research with special reference to human disease. Biochem. Biophys. Res. Commun. 396, 120–124 (2010). https://doi.org/10.1016/j.bbrc.2010.03.083 PMid:20494123

74. Arscott, L. D., Gromer, S., Schirmer, R. H., Becker, K. & Williams, C. H. The mechanism of thioredoxin reductase from human placenta is similar to the mechanisms of lipoamide dehydrogenase and glutathione reductase and is distinct from the mechanism of thioredoxin reductase from Escherichia coli. Proc. Natl. Acad. Sci. 94, 3621–3626 (1997). https://doi.org/10.1073/pnas.94.8.3621 PMid:9108027 PMCid:PMC20490

75. Zhong, L., Arnér, E. S. J. & Holmgren, A. Structure and mechanism of mammalian thioredoxin reductase: The active site is a redox-active selenolthiol/selenenylsulfide formed from the conserved cysteine-selenocysteine sequence. Proc. Natl. Acad. Sci. U. S. A. 97, 5854–5859 (2000). https://doi.org/10.1073/pnas.100114897 PMid:10801974 PMCid:PMC18523

76. Karran, P. & Attard, N. Thiopurines in current medical practice: molecular mechanisms and contributions to therapy-related cancer. Nat Rev Cancer 8, 24–36 (2008). https://doi.org/10.1038/nrc2292 PMid:18097462

77. Fieser, L. F. & Fieser, M. Reagents for Organic Synthesis. Louis F. Fieser and Mary Fieser. Wiley, New York, 1967. 1469 pp., illus. $27.50. Reag. Org. Synth. Louis F Fieser Mary Fieser Wiley N. Y. 668 (1968).

78. Hanna, N. B., Ramasamy, K., Robins, R. K. & Revankar, G. R. A convenient synthesis of 2'-deoxy-6-thioguanosine, and certain related purine nucleosides by the stereospecific sodium salt glycosylation procedure. J. Heterocycl. Chem. 25, 1899–1903 (1988). https://doi.org/10.1002/jhet.5570250653

79. Gao, L. et al. Gold(I) Styrylbenzene, Distyrylbenzene, and Distyrylnaphthalene Complexes: High Emission Quantum Yields at Room Temperature. Chem. – Eur. J. 18, 6316–6327 (2012). https://doi.org/10.1002/chem.201102502 PMid:22473678

80. Gao, L. et al. Mono- and Di-Gold(I) Naphthalenes and Pyrenes: Syntheses, Crystal Structures, and Photophysics. Organometallics 28, 5669–5681 (2009). https://doi.org/10.1021/om9005214

81. Partyka, D. V., Zeller, M., Hunter, A. D. & Gray, T. G. Relativistic functional groups: aryl carbon-gold bond formation by selective transmetalation of boronic acids. Angew. Chem. Int. Ed Engl. 45, 8188–91 (2006). https://doi.org/10.1002/anie.200603350 PMid:17111449

82. Heckler, J. E., Zeller, M., Hunter, A. D. & Gray, T. G. Geminally Diaurated Gold(I) Aryls from Boronic Acids. Angew. Chem. Int. Ed. 51, 5924–5928 (2012). https://doi.org/10.1002/anie.201201744 PMid:22565395

83. O'Brien, J., Wilson, I., Orton, T. & Pognan, F. Investigation of the Alamar Blue (resazurin) fluorescent dye for the assessment of mammalian cell cytotoxicity. Eur. J. Biochem. FEBS 267, 5421–6 (2000). https://doi.org/10.1046/j.1432-1327.2000.01606.x

84. Craig, S., Gao, L., Lee, I., Gray, T. & Berdis, A. J. Gold-Containing Indoles as Anticancer Agents That Potentiate the Cytotoxic Effects of Ionizing Radiation. J. Med. Chem. 55, 2437–2451 (2012). https://doi.org/10.1021/jm2005942 PMid:22289037 PMCid:PMC3326641

85. Holmgren, A. Thioredoxin structure and mechanism: conformational changes on oxidation of the active-site sulfhydryls to a disulfide. Structure 3, 239–243 (1995). https://doi.org/10.1016/S0969-2126(01)00153-8